Chapter 1

# Two-Photon Absorption in Photodiodes

Toshiaki Kagawa

Additional information is available at the end of the chapter

http://dx.doi.org/10.5772/50491

## 1. Introduction

Incident light with a photon energy $\hbar\omega$ induces two-photon absorption (TPA) when $E_g / 2\hbar\omega E_g$, where $E_g$is the band gap of the photo-absorption layer of a photodiode (PD). Because the absorption coefficient is small, photocurrent generated by TPA is too low to be used in conventional optical signal receivers. However, the nonlinear dependence of the photocurrent on the incident light intensity can be used for optical measurements and optical signal processing. It has been used for autocorrelation in pulse shape measurements [1], dispersion measurements [2,3] and optical clock recovery [4]. These applications exploit the dependence of the generated photocurrent on the square of the instantaneous optical intensity. Measurement systems using TPA in a PD can detect rapidly varying optical phenomena without using high speed electronics.

This chapter reviews research on TPA and its applications at the optical fiber transmission-wavelength. Theory of TPA for semiconductors with diamond and zinc-blende crystal structures is reviewed. In contrast to linear absorption for which the photon energy exceeds the band gap, the TPA coefficient depends on the incident lightpolarization. The polarization dependence is described by the nonlinear susceptibility tensor elements.

The polarization dependences of TPA induced by a single optical beam in GaAs- and Si-PDs are compared to evaluate the effect of crystal symmetry. It is found that, in contrast to the GaAs-PD, TPA in the Si-PD is isotropic for linearly polarized light at a wavelength of 1.55 μm. Photocurrents for circularly and elliptically polarized light are also measured. Ratios of the nonlinear susceptibility tensor elements are deduced from these measurements. The different isotropic properties of GaAs- and Si-PDs are discussed in terms of the crystal and band structures.

Cross-TPA between two optical beams is also studied. The absorption coefficient of cross-TPA strongly depends on the polarizations of the two optical beams. It is shown that the po-

larization dependence of cross-TPA is consistent with the nonlinear susceptibility tensor elements obtained from the self-TPA analysis.

Cross-TPA can be applied to polarization measurements. Photocurrents generated in the Si-PD by cross-TPA between asignal light under test and a reference light are used to detect the polarization. The light under test is arbitrarily polarized and its Jones vector can be determined by photocurrents generated by cross-TPA. This measurement method can detect the instantaneous polarization when the reference light temporally overlaps with the light under test. Because the time division is limited only by the pulse width of the reference light, it is possible to detect rapid variationsin the polarization. This method can measure not only the linear polarization direction but also the elliptical polarization. Applications to measurement of the output optical pulse from an optical fiber with birefringence and a semiconductor optical amplifier are demonstrated.

## 2. TPA in semiconductors with diamond and zinc-blende crystals

### 2.1. Polarization dependence

TPA is a third-order nonlinear optical process. Third order nonlinear polarization is induced by the optical electric field according to

$$P_i^{(3)}(\omega_i, \boldsymbol{k}_i) = \frac{1}{4}\varepsilon_0 \sum_{j,k,l} \chi_{ijkl} E_j(\omega_j, \boldsymbol{k}_j) E_k(\omega_k, \boldsymbol{k}_k) E_l(\omega_l, \boldsymbol{k}_l) \tag{1}$$

where$\varepsilon_0$ is the permittivity of free space, $\chi$ is the third-order tensor, $\omega$ is the optical angular frequency, k is the optical wavenumber vector, $E$ is the optical electric field [5]. The suffixes $i$, $j$, $k$, and $l$ denote the orthogonal directions. The relationships between the optical angular frequencies and the wavenumber vectors are determined by energy and momentum conservation, respectively.

Although the third-order nonlinear susceptibility tensor contains $3^4$ elements, the number of non-zero independent elements is limited by the crystal symmetry and the properties of the incident light. It is apparent that relations $\chi_{xxxx} = \chi_{yyyy} = \chi_{zzzz}$and $\chi_{xxyy} = \chi_{xxzz} = \chi_{yyzz}$, etc. hold for a cubic crystal. Elements like $\chi_{xxxy}$and$\chi_{xxyz}$will be zero for crystals with 180° rotational symmetry about a crystal axis. For degenerate TPA in which one or two parallel optical beams with the same optical frequency propagate,$\omega_i = -\omega_j = \omega_k = \omega_l$ and $\chi_{xyxy} = \chi_{xyyx}$ hold. There are thus only three independent elements, $\chi_{xxxx}$, $\chi_{xxyy}$, and $\chi_{xyyx,}$ for degenerate TPA in crystal classes of $m3m$ (Si) and $\bar{4}3m$ (GaAs) [5,6].

We consider cross- and self-TPA between two optical beams. The electric field is the sum of the electric fields of thetwo incident optical beams.

$$\boldsymbol{E} = E_p \hat{\boldsymbol{p}} + E_e \hat{\boldsymbol{e}} \tag{2}$$

where $E_p$ and $E_e$ are the electric field strengths and $\hat{\boldsymbol{p}}$ and $\hat{\boldsymbol{e}}$ are the polarization unit vectors of the two beams. For circular or elliptical polarization, $\hat{\boldsymbol{p}}$ and $\hat{\boldsymbol{e}}$ are complex to express the phase difference between the electric field oscillations along two axes. The nonlinear polarization along the polarization vector $\hat{\boldsymbol{p}}$ is given by

$$P_p^{(3)} = \frac{1}{4}\varepsilon_0 (E_p^3 \sum_{i,j,k,l} p_i^* p_j^* p_k p_l \chi_{ijkl} + 2E_p E_e^2 \sum_{i,j,k,l} p_i^* e_j^* p_k e_l \chi_{ijkl}) \tag{3}$$

where $p_i$ and $e_i$ are elements of $\hat{\boldsymbol{p}}$ and $\hat{\boldsymbol{e}}$, and $p_i^*$ and $e_i^*$ are their complex conjugate, respectively. Because there are only three nonzero independent tensor elements, the nonlinear polarization can be written as [7]

$$\begin{aligned} P_p^{(3)} = \frac{1}{4}\varepsilon_0 \Big\{ & E_p^3 (|\hat{\boldsymbol{p}} \cdot \hat{\boldsymbol{p}}|^2 \cdot \chi_{xxyy} + 2\chi_{xyyx} + \sigma \chi_{xxxx} \sum_i |p_i|^4) \\ & + 2E_p E_e^2 (\chi_{xxyy} |\hat{\boldsymbol{p}} \cdot \hat{\boldsymbol{e}}|^2 + \chi_{xyyx}(1 + |\hat{\boldsymbol{p}}^* \cdot \hat{\boldsymbol{e}}|^2) + \sigma \chi_{xxxx} \sum_i |p_i|^2 |e_i|^2) \Big\} \end{aligned} \tag{4}$$

where

$$\sigma = \frac{\chi_{xxxx} - \chi_{xxyy} - 2\chi_{xyxy}}{\chi_{xxxx}} \tag{5}$$

The first and second terms are polarization induced by the self- and cross-electric field effects, respectively. Terms proportional to the inner product of $\hat{\boldsymbol{p}}$ and $\hat{\boldsymbol{e}}$ are invariant for rotation of axes and are isotropic. In contrast, terms that are proportional to $\sigma$ vary on the rotation of the axes. Thus, $\sigma$ shows the anisotropy of the third-order nonlinear optical process.

Two optical beams propagate in the crystal under the effect of self- and cross-TPA.

$$\frac{dI_p}{dz} = -\beta_{pp} I_p^2 - \beta_{pe} I_p I_e \tag{6}$$

where $I_p$ and $I_e$ are optical intensity densities of the two beams. The absorption coefficient is proportional to the imaginary part of the nonlinear polarization given in Eq. (4).

$$\beta_{pp} = \frac{\omega}{2n^2c^2\varepsilon_0}(\chi''_{xxyy} \mid \hat{\boldsymbol{p}} \cdot \hat{\boldsymbol{p}} \mid^2 + 2\chi''_{xyyx} + \sigma''\chi''_{xxxx}\sum_i \mid p_i \mid^4) \tag{7}$$

and

$$\beta_{pe} = \frac{\omega}{n^2c^2\varepsilon_0}(\chi''_{xxyy} \mid \hat{\boldsymbol{p}} \cdot \hat{\boldsymbol{e}} \mid^2 + \chi''_{xyyx}(1 + \mid \hat{\boldsymbol{p}}^* \cdot \hat{\boldsymbol{e}} \mid^2) + \sigma''\chi''_{xxxx}\sum_i \mid p_i \mid^2 \mid e_i \mid^2) \tag{8}$$

where $n$ is the refractive index, and $c$ is the speed of light. $\chi''_{xxxx}$etc. are imaginary parts of the nonlinear susceptibility tensor elements. $\sigma''$is the anisotropy parameter for imaginary parts of the nonlinear susceptibility tensor.

$$\sigma'' = \frac{\chi''_{xxxx} - \chi''_{xxyy} - 2\chi''_{xyyx}}{\chi''_{xxxx}} \tag{9}$$

### 2.2. Estimate of photocurrent induced by TPA in PDs

Commercially available PDs are usually designed to be used for photon energies greater than the band gap of the photoabsorption layer. As the absorption coefficient is about $10^5$ $cm^{-1}$, absorption layer is several micrometers thick. On the other hand, the absorption coefficient is much smaller for TPA. If we consider only self-TPA, Eq. (6) is solved as

$$I_p(z) = \frac{I_0}{\beta_{pp}I_0z + 1} \approx I_0(1 - \beta_{pp}I_0z) \tag{10}$$

where $I_0$ is the initial light intensity density. Using a typical value of $10^{-18}$ $m^2/V^2$ for the imaginary parts of the nonlinear susceptibility tensor elements [7], the TPA coefficient is estimated to be about $6 \times 10^{-11}$ m/W. When the incident light density is $10^7$ W/$cm^2$, $\beta_{pp} I_0$is estimated to be$6 \times 10^{-6}$μ$m^{-1}$. Because only a very small fraction of the incident light is absorbed in PD with a photo-absorption layer that is several micrometers thick, the induced photocurrent is proportional to the absorption coefficient $\beta$.

When optical pulses with an intensity density $I_0$ and pulse width $T_p$are irradiated at a repetition rate of $R$, the induced photocurrent will be

$$J = \eta\beta_{pp}I_0^2 S\, d\, T_p R\, \frac{q}{\hbar\omega} \tag{11}$$

where $\eta$ is the internal efficiency of the PD, $d$ is the absorption layer thickness, and $S$ is the area of the incident beam. The photocurrent is estimated to be about $10^{-8}$ A assuming that

the light intensity of $10^7$ W/cm$^2$ is illuminated on a spot with adiameter of 10 μm. We assume that the pulse width is 1 ps, the repetition rate is 100 MHz, absorption layer thickness is 2 μm, and the internal efficiency is 1.

## 3. Experimental setup

Because the photocurrent of PD is proportional to the square of the instantaneous light power density, it is necessary to concentrate the optical power into a narrow spatial region and a short time period. Thus, a short pulsed light beam is more suitable for TPAmeasurementsthan continuous wave light.

Figure 1 shows the experimental setup. A gain-switched laser diode (LD) generated optical pulses with a wavelength of 1.55 μm, a pulse width of 50 ps and a repetition rate of 100 MHz. Light pulse from the gain-switched LD exhibit large wavelength chirping. The pulse was compressed to about 10 ps by an optical fiber with positive wavelength dispersion. Its peak power was then amplified using an Er-doped fiber amplifier (EDFA) to further compress the pulse width through the nonlinear soliton effect in a normal-dispersion fiber. The final pulse width was compressed toabout 1 ps.

To measure cross-TPA between two optical beams, a second gain switched LD with a wavelength of 1.55 μm was prepared. Noise due to interference between the two beams does not affect the measurement because the optical frequency difference between the two beams is greater than the bandwidth of the measurement system. Pulse with a repetition rate of 100MHz are completely synchronized with those of the first optical beam. The second optical beam is also amplified by an EDFA.

Both the two beams were made linearly polarized by polarization controllers. After they were launched into free space, they passed through polarizing beam splitters to ensure that they were completely linearly polarized. Half-wave or quarter-wave plates were inserted if it is necessary to control the polarization of the beams. The two beams were spatially overlapped by a polarization-independent beam splitter and they were focused on a PD. It was confirmed that the polarization did not change on reflection at the polarization-independent beam splitter by monitoring the polarization before and after reflection. An optical power meter was placed at the location of the PD and it was used to check if the optical power was independent of the polarization.

When two optical beams are illuminated on a PD, photocurrents due to self-TPA and cross-TPAare simultaneously generated. It is necessary to detect only the photocurrent generated by the cross-TPA. Optical pulse streams were mechanically chopped at frequencies of 1.0 and 1.4 kHz. Electrical pulsesthat had been synchronized with mechanical choppers were fed into a mixer circuit that generated a sumfrequency of 2.4 kHz. These generated electrical pulses with the sum frequency were used as the reference signal for the lock-in amplifier. Thus, the lock-in amplifier detected only the photocurrent generated by two-beam absorption, that is, cross TPA.

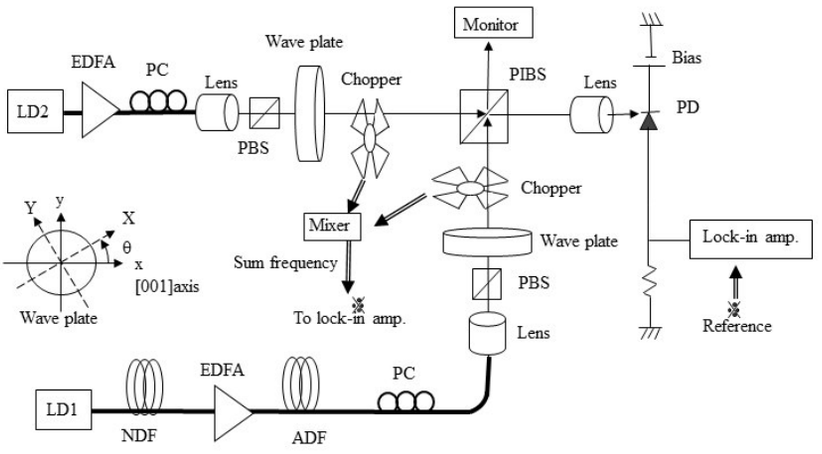


**Figure 1.** Measurement setup (LD: laser diode; NDF: normal dispersion fiber; ADF: abnormal dispersion fiber; PBS: polarization beam splitter; PIBS: polarization independent beam splitter). The inset shows the rotation of the wave plate. Light from the PBS is linearly polarized along the *x* axis,which is parallel tothe [1] axis of the PD.

## 4. Pulse width measurement by cross-TPA

Cross-TPA was used to measure the pulse width generated by the pulse compression process described in the previous section. After the compressed optical pulse was divided into two branches by an optical fiber beam splitter, the timing between them was controlled by a variable delay line. They were then irradiated on the Si-PD. The two beams were made orthogonally linearly polarized to suppress noise due to interference. The photocurrent generated by cross-TPA between the divided two optical beams is

$$J(\tau)=\beta\int h(t)h(t-\tau)dt \tag{12}$$

where $h(t)$ is the pulse shape, and $\tau$ is the time delay between the two pulses. The pulse width can be estimated by this self-correlation trace.

Figure 2 shows the self-correlation trace of the compressed optical pulse. The photocurrent due to the cross-TPA is generated only when the two optical pulses temporally overlap on the PD. It disappears when the time delay is larger than the pulse width. The self-correlation trace has a full-width at half-maximum (FWHM) of 1.3 ps. The FWHM of the pulse is estimated to be about 0.9 ps assuming a Gaussian pulse shape.

## 5. Polarization dependence of self-TPA in Si- and GaAs-PDs

Measuring the photocurrent generated in PDs is the easiest way to study the polarization dependence of self-TPA coefficient. Because the fraction of the incident photons that are ab-

sorbed is quite small, the generated photocurrent is directly proportional to the absorption coefficient$\beta_{pp}$as shown by Eq. (10). The photocurrents generated in Si- and GaAs-PDs were compared to discuss the polarization dependence of TPA in Si and GaAscrystals[8].

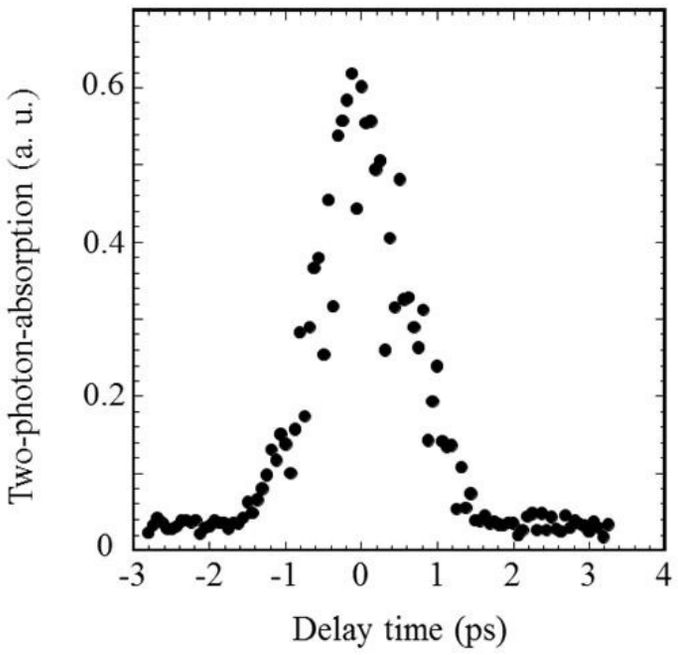


**Figure 2.** Self-correlation trace of the compressed pulse measured by TPA of Si-PD.

In the self-TPA measurement, only one optical beam is illuminated on a PD. The optical beam with a pulse width of 0.9 ps in the measurement setup described in section 3was used in the self-TPAmeasurement. The x- and y- axes are fixed in the laboratory frame. We consider the case when light that is linearly polarized alongthe $x$-axis is transformed by a half- or quarter-wave plate. The principal axis of the wave plate is rotated at an angle of $\theta$ relative to the $x$-axis. The polarization of the transformed light is expressedby

$$\hat{\boldsymbol{p}}=\begin{pmatrix}p_x\\p_y\end{pmatrix}=\begin{pmatrix}\cos\theta & -\sin\theta\\ \sin\theta & \cos\theta\end{pmatrix}\begin{pmatrix}1 & 0\\ 0 & e^{i\varphi}\end{pmatrix}\begin{pmatrix}\cos\theta & \sin\theta\\ -\sin\theta & \cos\theta\end{pmatrix}\begin{pmatrix}1\\0\end{pmatrix} \tag{13}$$

where $\phi=\pi$ and $\pi/2$ for half- and quarter-wave plates, respectively. The inset of Fig. 1 shows the definition of the rotation angle. The principal axes of the quarter-wave plate are represented by the $X$- and $Y$-axes. The phase of the polarization component along the $Y$-axis is delayed by $\phi$ relative to that along the $X$-axis.

The anisotropy of self-TPA for linearly polarized light was measured for Si- and GaAs-PDs. The crystal axis [001] is made parallel to the x-axis. The linear polarization is rotated by a half-wave plate (i.e., $\phi=\pi$ in Eq. (13)). When the X-axis is tilted by an angle of $\theta$ relative to the $x$-axis, the polarization direction of the output light from the half-wave plate is tilted by

$2\theta$. Thus, the polarization is parallel to the [001] and [011] directions when the rotation angle of the half-wave plate is $\theta$ = 0 and 22.5° , respectively. Using Eq. (7), the anisotropy parameter $\sigma''$ defined by Eq. (9) can be written as

$$\sigma'' = 2\frac{\beta_{pp}{}^{L}[001] - \beta_{pp}{}^{L}[011]}{\beta_{pp}{}^{L}[001]} \tag{14}$$

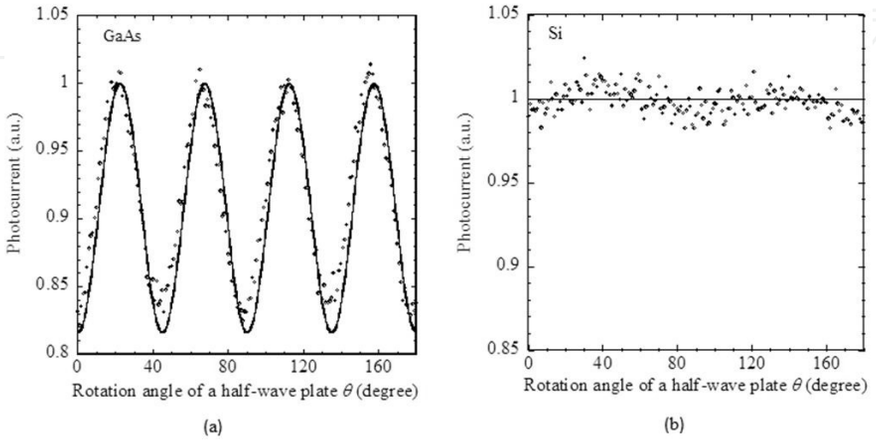


**Figure 3.** Photo currents generated when linearly polarized lightirradiated on (a) GaAs PD and (b) Si PD. The linear polarization direction is rotated using a half-wave plate. The horizontal axis is the tilt angle of the half wave plate.The solid lines in (a) and (b) show the values calculated using Eq. (15) with $\sigma''$ = –0.45 and 0, respectively.

where$\beta_{pp}{}^{L}[001]$ and $\beta_{pp}{}^{L}[011]$ are the TPA coefficients for linearly polarized light polarized along the [001] and [011] directions, respectively.This parameter can be experimentallydetermined by the ratio of photocurrents.

Figures 3(a) and (b) respectively show the photocurrents generated in GaAs- and Si-PD sas a function of the rotation angle of the half-wave plate. For the GaAs-PD, the photocurrent varies with the polarization direction indicating that the TPA is anisotropic. The anisotropy parameter $\sigma''$ is estimated to be –0.45. From Eqs. (7), (9) and (13), the dependence of the TPA probability on the rotation angle $\theta$of the half-wave plate can be written as

$$\beta_{pp}{}^{L} \propto \frac{1}{4}\chi''_{xxxx}(4 - \sigma'' + \sigma''\cos 8\theta) \tag{15}$$

The solid line in Fig. 3 (a) shows the value calculated using Eq. (15) and $\sigma''$= –0.45. In contrast, the Si-PD exhibits negligibly small dependence on the polarization direction and the TPA coefficient is almost isotropic; $|\sigma''|$ is estimated to be less than 0.04.

Figure 4(a) and (b) respectively shows the dependence of the photocurrents generated in the GaAs- and Si-PDs on the rotation angle of a quarter-wave plate ($\phi$=$\pi$/2in Eq. (13)). The incident light is linearly polarized along the [001] direction and circularly polarized at $\theta$ = 0 and

45° , respectively. The difference in the self-TPA coefficients for linear and circular polarization isexpressed by the dichroism parameter

$$\delta = \frac{\beta_{pp}{}^{L}[001] - \beta_{pp}{}^{C}}{\beta_{pp}{}^{L}[001]} = \frac{\chi''_{xxxx} + \chi''_{xxyy} - 2\chi''_{xyyx}}{2\chi''_{xxxx}} \tag{16}$$

where$\beta_{pp}{}^{C}$ is the TPA coefficient for circularly polarized light. This parameter is estimated to be 0.1 and 0.39 from the measured photocurrents for linearly and circularly polarized light in the GaAs- and Si-PD, respectively.

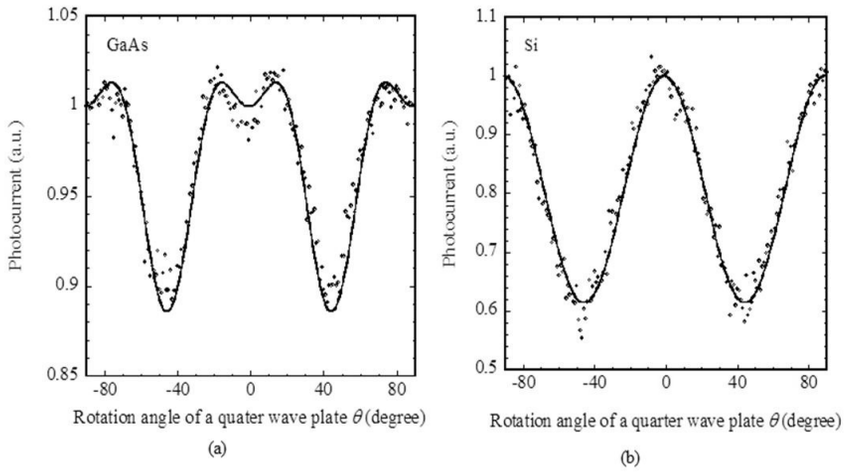


**Figure 4.** Photocurrent obtained when elliptically polarized light is incident on (a) GaAs and (b) Si PDs. Linearly polarized light along the [001] axis is transformed by a quarter-wave plate rotated at an angle of $\theta$.The solid lines indicate the results calculated using Eq. (17) and the parameters in Table 1.

The ratios $\chi''_{xxyy}/\chi''_{xxxx}$ and $\chi''_{xyyx}/\chi''_{xxxx}$ can be estimated from measured anisotropic and dichroism parameters. Table 1 lists the obtained ratios for the nonlinear susceptibility tensor elements for GaAs and Si.

From Eqs. (7), (9), (13) and (16), the dependence of the TPA coefficient on the quarter-wave plate rotation angle $\theta$ is given by

$$\beta_{pp} \propto \frac{1}{16}\chi''_{xxxx}(16 - \sigma'' - 8\delta + \sigma''\cos 8\theta + 8\delta\cos 4\theta) \tag{17}$$

This self-TPA coefficient is maximized when

$$\cos^2 2\theta = -\frac{\chi''_{xxyy}}{\chi''_{xxxx}}\frac{1}{\sigma''} \tag{18}$$

The absorption coefficient for this elliptically polarized light is greater than$\beta^{L}[001]$.

The solid lines in Figs. 4(a) and (b) show the results calculated using Eq. (17) for GaAs and Si, respectively. The photocurrent shown in Fig. 4(a) reaches a maximum at $\theta = 15°$ , which indicates that Eq. (18) holds at this angle. The factor $\chi''_{xxyy} / (\sigma'' \chi''_{xxxx})$ in Eq. (18) is estimated to be –0.75 for GaAs. This value is consistent with the values of $\sigma''$ and $\chi''_{xxyy} / \chi''_{xxxx}$ in Table 1, indicating that the polarization dependence of the GaAs-PD is consistent with the analysis based on the nonlinear susceptibility.

On the other hand, the photocurrent generated in the Si-PD is maximized when the angle is 0 and the incident light is linearly polarized, which contrasts the situation for the GaAs PD. Because the anisotropy parameter is small, Eq. (18) does not hold at any rotation angle $\theta$.

## 6. Discussion of self-TPA polarization dependence

The polarization dependence of self-TPA is strongly dependent on the crystal symmetry and the band structure. Hutchings and Wherettcalculated nonlinear susceptibility tensor elements based on kp perturbation [9]. The ratios listed in Table 1 are consistent with their results. Murayamaand Nakayama[10] have performed *ab initio* calculations.Their calculated values for the ratios $\chi''_{xxyy} / \chi''_{xxxx}$ and $\chi''_{xyyx} / \chi''_{xxxx}$ depend on the photon energy. The values of ratios shown in Table 1 are very similar to those calculated for a photon energy of 1 eV. The small discrepancy between the photon energies is probably due to the parameters used in the calculation.

| | GaAs | Si |
|---|---|---|
| Anisotropy parameter $\sigma''$ | -0.45 | $\lvert\sigma''\rvert < 0.04$ |
| Dichroism parameter $\delta$ | 0.1 | 0.39 |
| $\chi''_{xxyy} / \chi''_{xxxx}$ | 0.34 | 0.39 |
| $\chi''_{xyyx} / \chi''_{xxxx}$ | 0.56 | 0.31 |

**Table 1.** Parameters obtained from the polarization dependence of the photocurrents of GaAs and Si PDs at a wavelength of 1.55 μm.

It is very reasonable that GaAs and Si were observed to have quite different anisotropies because of their different crystal symmetries and band structures. As GaAs has a direct transition type band structure, an optical transition occurs at around the Γ point. The anisotropy for GaAs is due to the allowed–allowed transition [7,9] (see Fig. 5(a)), which is the two-step optical transition of $\Gamma_{15v} \rightarrow \Gamma_{15c} \rightarrow \Gamma_{1c}$. $\Gamma_{15v}$, $\Gamma_{1c}$, and $\Gamma_{15c}$ are irreducible representations of the point group $T_d(\bar{4}3m)$ of the GaAs crystal for the highest valence band, the lowest conduction band, and the higher conduction band at the Γ point, respectively [11]. The first transition $\Gamma_{15v} \rightarrow \Gamma_{15c}$ occurs between p-like states, the second transition $\Gamma_{15c} \rightarrow \Gamma_{1c}$ occurs between p-like

and s-like states. The polarization directions that induce the first and second transitions must be different from each other. For example, transitions $|p_z(\Gamma_{15v})\rangle \rightarrow |p_x(\Gamma_{15c})\rangle$ and $|p_x(\Gamma_{15c})\rangle \rightarrow |s(\Gamma_{1c})\rangle$ are induced by dipole moments polarized along the*y*- and *x*-axes, respectively. $|p_z(\Gamma_{15v})\rangle$, $|p_x(\Gamma_{15c})\rangle$,and $|s(\Gamma_{1c})\rangle$ are wave functions of each band [11]. This process does not contribute to $\chi''_{xxxx}$and$\chi''_{xxyy}$, but it contributes to $\chi''_{xyyx}$causing the anisotropy parameter σ'' to be non-zero [7]. The matrix element of the optical dipole moment between $\Gamma_{15v}$ and $\Gamma_{15c}$ is non-zero because $T_d$ lacks space inversion symmetry.

On the other hand, Si has the indirect transition type band structure. Figure 5(b) schematically shows the band structure and the irreducible representation of this space group [11,12]. A photon energy of 0.8 eV is too small to induce a direct TPA transition without phonon absorption or emission at any point in the first Brillouin zone of Si. The final sate of the TPA transition is $\Delta_1$, which has the minimum energy of the conduction band. Many complicated transitionsequences that include optical and phonon transitions exist to reach the final point $\Delta_1$ for electron.

When both optical transitions occur at Γ point, an electron is scattered to $\Delta_1$in the conduction band. However, two step optical transitions in Si are quite different from that in GaAs. Si crystal has a point group of $O_h(m3m)$ that has space inversion symmetry and the wavefunction is an eigenstate of the parity at the Γ point. The matrix elements of the dipole moment between the conduction bands of $\Gamma_{15}$, $\Gamma_{2'}$, and $\Gamma_{12'}$ vanish because they all have the same parity. The only possible virtual final state of the two-step optical transition sequence in Γ point is $\Gamma_1$ in the higher conduction band. As$\Gamma_1$ has a much greater energy than $\Gamma_{25'}$ and$\Delta_1$, the transition probability is thought quite small.

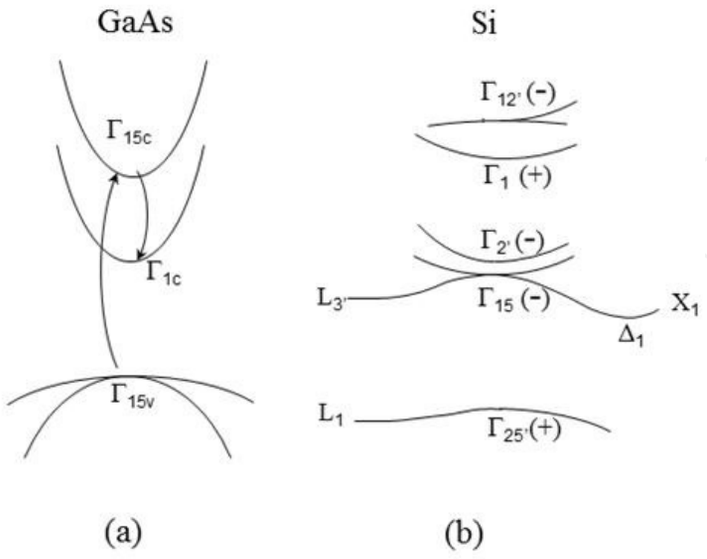


**Figure 5.** a) Schematic band structure and allowed–allowed transition in GaAs. (b) Schematic band structure of Si

When a phonon process occurs after the first optical transition, the polarization effect of the first optical transition on the intermediate state of TPA can be destroyed by the phonon process. The anisotropy is thus considered to be reduced by this process.

## 7. Cross-TPA in Si-APD

As shown in the previous section, TPA in Si is isotropic. Thus, TPA in Si-PD is simpler than that in GaAs-PD. In addition, a Si avalanche photodiode (APD) with the multiplication gain is commercially available. Consequently, we concentrate on cross-TPA in Si-APD.

Cross-TPA depends on the relationship between the polarization vectors of the two beams. We measure three cases: when both beams are linearly polarized, when one optical beam is linearly polarized and the other is varied between linear, elliptical, and circular polarization by a quarter-wave plate, and when one beam is circularly polarized and the other is varied between linear, elliptical, and circular polarization [13].

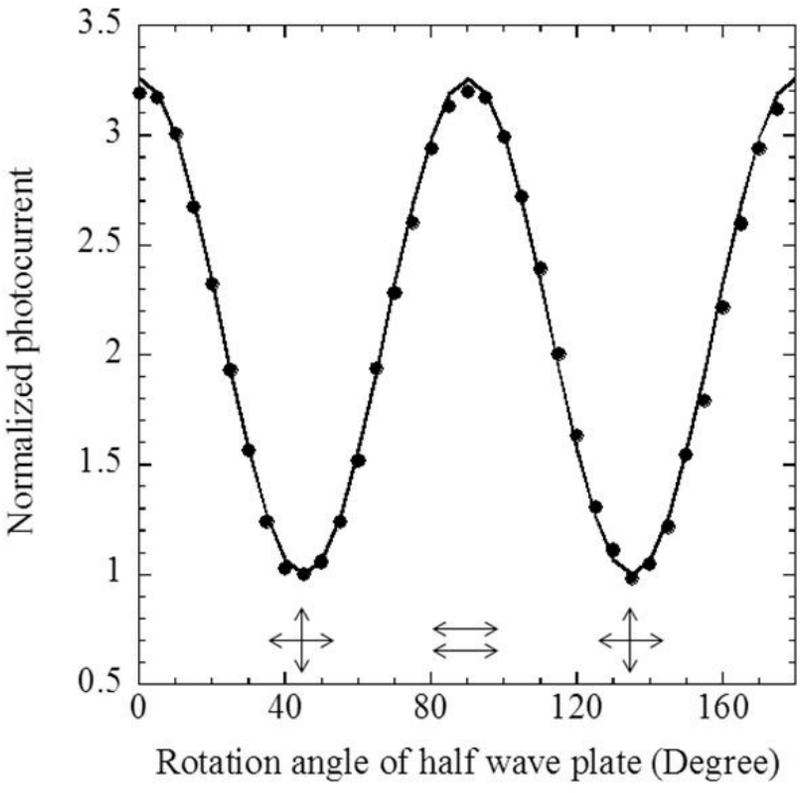


**Figure 6.** Photocurrent due to cross- TPA between two linearly polarized beams. Solid line is the calculated results using parameters in Table 1.

Figure 6 shows the photocurrent when both beams are linearly polarized. The horizontal axis of the figure is the rotation angle of the half- wave plate. The photocurrent was

normalized using the minimum photocurrent. The photocurrent is strongly dependent on the orientation of the two linear polarization axes and has a maximum and minimum values when the polarization axes of the two optical pulses are parallel and perpendicular, respectively.

Equation (8) can be written as

$$\beta_{pe} \propto \frac{1}{2}(\chi''_{xxyy} + \chi''_{xyyx})\cos 4\theta + \frac{1}{2}(\chi''_{xxyy} + 3\chi''_{xyyx}) \tag{19}$$

The solid line in Fig.6 shows the result calculated using Eq. (19) and the parameters in Table 1.

The absorption coefficient hasa maximum and minimum when $\hat{\boldsymbol{p}}$ and $\hat{\boldsymbol{e}}$ are parallel and orthogonal, respectively. The ratio of the maximum to minimum values is

$$\frac{\beta_{pe}(\hat{\boldsymbol{p}} // \hat{\boldsymbol{e}})}{\beta_{pe}(\hat{\boldsymbol{p}} \perp \hat{\boldsymbol{e}})} = 2 + \frac{\chi''_{xxyy}}{\chi''_{xyyx}} \tag{20}$$

Using the parameters in Table 1 which were obtained from the self-TPA of Si, this ratio is 3.26. This value is consistent with the measured cross-TPA shown in Fig 6..

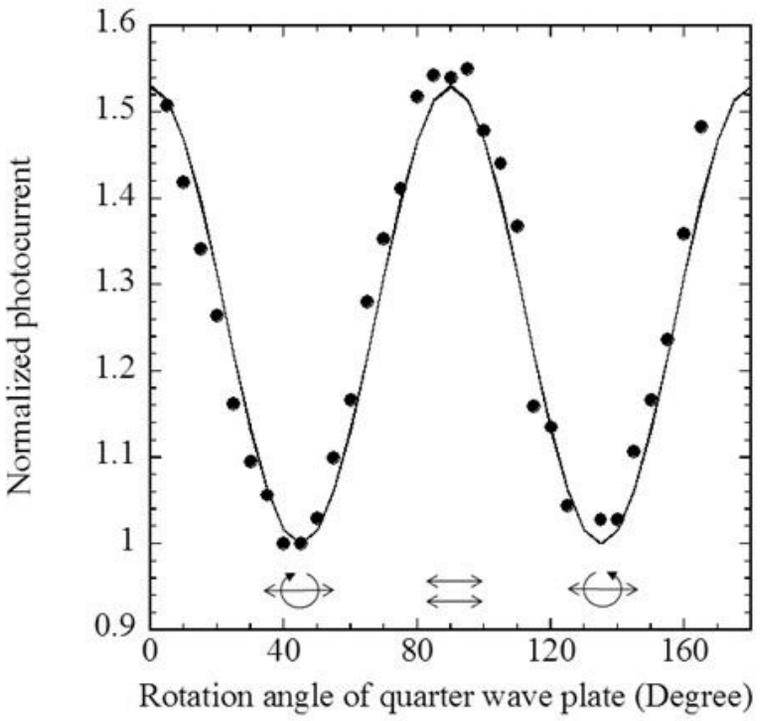


**Figure 7.** Photocurrent due to cross-TPA between linear polarized and elliptical polarized lights. Solid line is the calculated results using parameters in Table 1.

Figure 7 shows the photocurrent when one beam ($\hat{\boldsymbol{e}}$) was linearly polarized and the polarization of the other beam ($\hat{\boldsymbol{p}}$) was varied using a quarter-wave plate. The horizontal axis is the rotation angle of the quarter-wave plate. The polarization of the second beam varied between linear, elliptical, and circular in this case. The solid line shows the calculated value using the parameters in Table 1. The photocurrent had maximum and minimum values when the second beam was linearly and circularly polarized, respectively. The ratios are theoretically written as

$$\frac{\beta_{pe}(\hat{\boldsymbol{p}}//\hat{\boldsymbol{e}})}{\beta_{pe}(\hat{\boldsymbol{p}};circular)}=\frac{4+2\chi''_{xxyy}/\chi''_{xyyx}}{3+\chi''_{xxyy}/\chi''_{xyyx}} \tag{21}$$

using Eq (8). This ratio is calculated to be 1.53 from the parameters in Table 1, and is consistent with the measurement.

Figure 8 shows the photocurrent when one beam was circularly polarized while the polarization of the other beam was varied using a quarter-wave plate between linear, elliptical, and circular polarization. The unit vectors for circular polarization are $\hat{\boldsymbol{\sigma}}_{+}=\frac{1}{\sqrt{2}}(\hat{\boldsymbol{x}}+i\hat{\boldsymbol{y}})$and $\hat{\boldsymbol{\sigma}}_{-}=\frac{1}{\sqrt{2}}(\hat{\boldsymbol{x}}-i\hat{\boldsymbol{y}})$. An arbitrary polarization vector $\hat{\boldsymbol{p}}$ can be written as a linear combination of these unit vectors.

$$\hat{\boldsymbol{p}}=p_{+}\hat{\boldsymbol{\sigma}}_{+}+p_{-}\hat{\boldsymbol{\sigma}}_{-} \tag{22}$$

When$\hat{\boldsymbol{e}}=\hat{\boldsymbol{\sigma}}_{-}$, Eq (8) can be written as

$$\beta_{pe}\propto\chi''_{xxyy}\mid p_{+}\mid^{2}+\chi''_{xyyx}(1+\mid p_{-}\mid^{2}). \tag{23}$$

We used the relations $\hat{\boldsymbol{\sigma}}_{+}\cdot\hat{\boldsymbol{\sigma}}_{-}=1$and$\hat{\boldsymbol{\sigma}}_{+}\cdot\hat{\boldsymbol{\sigma}}_{+}=\hat{\boldsymbol{\sigma}}_{-}\cdot\hat{\boldsymbol{\sigma}}_{-}=0$. $\beta_{pe}$ is independent of $\hat{\boldsymbol{p}}$ when $\chi''_{xxyy}=\chi''_{xyyx}$ because $\mid p_{+}\mid^{2}+\mid p_{-}\mid^{2}=1$.The photocurrent depends on the polarization, as Fig. 8 shows, but this dependence is relatively small.

The dependence of the absorption coefficient on the rotation angle is

$$\beta_{pe}\propto(\chi''_{xxyy}-\chi''_{xyyx})\sin2\theta+\chi''_{xxyy}+3\chi''_{xyyx} \tag{24}$$

The ratio of the maximum tominimum values is

$$\frac{\beta_{pe}(\hat{\boldsymbol{p}}=\hat{\boldsymbol{\sigma}}_{+})}{\beta_{pe}(\hat{\boldsymbol{p}}=\hat{\boldsymbol{\sigma}}_{-})}=\frac{1}{2}(1+\frac{\chi''_{xxyy}}{\chi''_{xyyx}}) \tag{25}$$

It is estimated to be 1.13 using the parameters in Table 1.

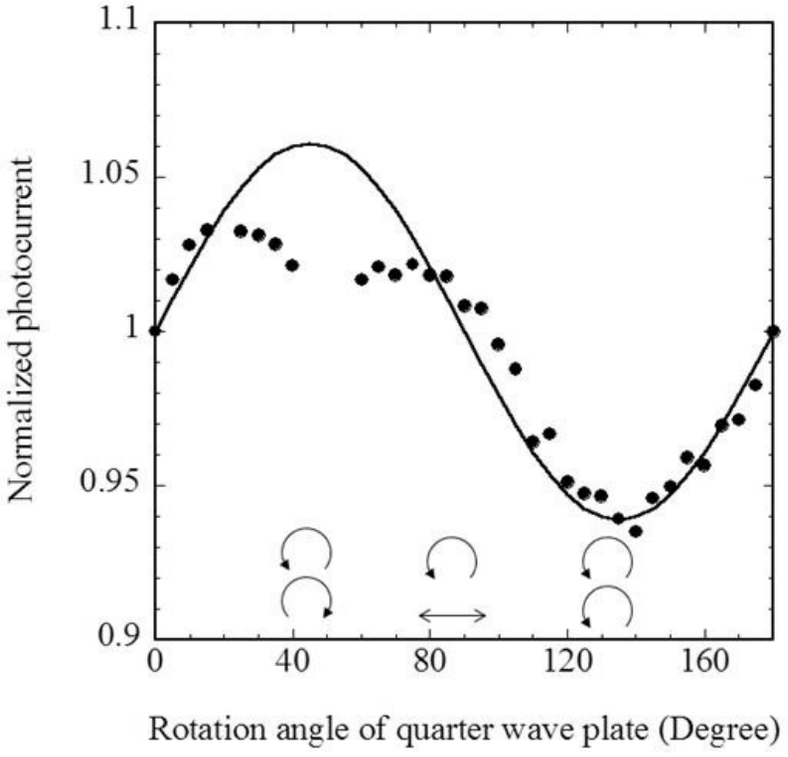


**Figure 8.** Photocurrent due to cross TPA when one optical beam is circularly polarized.

The solid line in Fig. 8 is the calculated results using Eq. (24). When one optical beam is circularly polarized, cross-TPA exhibits very weak dependences on the polarization of the other optical beam because values of $\chi''_{xxyy}$ and $\chi''_{xyyx}$ are very close to each other: however, in principle, they are not exactly equal for Si.

The calculated values shown by the solid lines in Figs. 6, 7, and 8 are obtained by nonlinear susceptibility tensor elements that were deduced from the polarization dependence of self-TPA. There is relatively good agreement with the measured cross-TPA. This demonstrates that the polarization dependences of self- and cross-TPA of Si are consistent with theoretical analysis based on the nonlinear susceptibility tensor.

## 8. Polarization measurement by cross-TPA

The polarization dependence of the cross-TPA in Si-APD can be used to measure the polarization. In this method, a Si-APD is irradiated by the arbitrarily polarized light to be measured (signal light) and a linearly polarized referencebeam. The photocurrents generated by cross-TPA between the signal light and the linearly polarized reference light are measured. Polarization direction of the reference beam was varied in four ways. Polarization of the arbitrarily polarized light can be determined from the four photocurrents of the APD [14].

Several applications require the ability to detect rapid variations in the polarization of an optical signal. In all conventional polarization measurement methods, the temporal resolu-

tion is limited by the response speed of the PD and/or electrical devices employed. Measurements based on TPA can be employed to measure rapidly varying polarization without the need to use high-speed electronics. Since the reference beam can be short pulses, the temporal polarization of a short-time period can be measured using this method. The temporal resolution is limited by only the pulse width of the reference light.

### 8.1. Principle of polarization measurement

The polarization of thelight to be measured can be generally described by the Jones vector

$$\hat{\boldsymbol{p}} = \begin{pmatrix} a_x \\ a_y e^{i\alpha} \end{pmatrix} \tag{26}$$

where $a_x$ and $a_y$ are respectively the amplitudes of the components in the $x$- and $y$-directions, and $\alpha$ is their phase difference. These three parameters are generally functions of time.The referencelight is linearly polarized and its Jones vector is given by

$$\hat{\boldsymbol{e}} = \begin{pmatrix} \cos\gamma \\ \sin\gamma \end{pmatrix} \tag{27}$$

where $\gamma$ expresses the polarization direction. The polarization of the reference lightis independent of time.

Let us consider four different polarization orientations of the linearly polarized reference light beam, namely, $\gamma_1 = 0$, $\gamma_2 = \pi/2$, $\gamma_3 = \pi/4$, and $\gamma_4 = \pi/4$.In the experiment, four photocurrents due to the cross TPA between the signal light and these four linearly polarized referencebeams are measured by a lock-in amplifier. From Eq. (8), the cross-TPA probability, which is proportional to the measured photocurrent, is given by

$$\beta_1(\gamma = 0) \propto a_x^2(\chi''_{xxyy} + \chi''_{xyyx}) + \chi''_{xyyx} \tag{28}$$

$$\beta_2(\gamma = \pi/2) \propto a_y^2(\chi''_{xxyy} + \chi''_{xyyx}) + \chi''_{xyyx} \tag{29}$$

$$\begin{aligned} \beta_3(\gamma = \pi/4) &\propto a_x a_y \cos\alpha\,(\chi''_{xxyy} + \chi''_{xyyx}) \\ &+ (\chi''_{xxyy} + 3\chi''_{xyyx})/2 \end{aligned} \tag{30}$$

$$\begin{aligned} \beta_4(\gamma = -\pi/4) &\propto -a_x a_y \cos\alpha\,(\chi''_{xxyy} + \chi''_{xyyx}) \\ &+ (\chi''_{xxyy} + 3\chi''_{xyyx})/2 \end{aligned} \tag{31}$$

Thus, the parameters of the measured light are given by

$$a_x{}^2 = \frac{x + 2 - \beta_2/\beta_1}{(x+1)(1+\beta_2/\beta_1)} \tag{32}$$

$$a_y{}^2 = 1 - a_x{}^2 \tag{33}$$

$$\cos\alpha = \frac{(x+3)(1-\beta_4/\beta_3)}{2a_x a_y (x+1)(1+\beta_4/\beta_3)} \tag{34}$$

$$x \equiv \chi''_{xxyy} / \chi''_{xyyx} \tag{35}$$

The polarization can be determined from the ratios of the photocurrent $\beta_2/\beta_1$ and $\beta_4/\beta_3$. $x$ is the ratio of the two independent non-diagonal elements of the third-order nonlinear susceptibility tensor; it was estimated to be 1.3 using values in Table 1. However, it was found that $a_x$, $a_y$, and $\alpha$are quite insensitive to $x$.

Let us consider the case when the pulse width of the reference light is much shorter than that of the light to be measured. The measured photocurrent produced by APD due to cross-TPA samples the polarization of the light being measured during the reference light pulse. It is thus possible to measure polarization as a function of time by varying the timing of the short reference light pulse.

One problem with this measurement method is that the sign of sin$\alpha$ cannot be determined as long as the reference light is linearly polarized. When it is important to determine the sign ofsin$\alpha$, it is necessary to compare the two photocurrents generated by cross-TPA for right and left circularly polarized localized lights; let us define these absorption coefficients as

$$\beta_5(\hat{\boldsymbol{e}} = \frac{1}{\sqrt{2}}\begin{pmatrix}1\\ i\end{pmatrix}) \tag{36}$$

and

$$\beta_6(\hat{\boldsymbol{e}} = \frac{1}{\sqrt{2}}\begin{pmatrix}1\\ -i\end{pmatrix}) \tag{37}$$

respectively. The sign of sin$\alpha$ is positive when $\beta_6 > \beta_5$and vice versa.

### 8.2. Measurement of stationary polarization

Polarization measurements were performed using the same setup as that shown in Fig. 1. The reference light is linearly polarized and its polarization direction $\gamma$ was varied in four ways by a half- wave plate. On the other hand, for the signal light, linear polarization was

transferred to linear, elliptical, and circular polarization by a quarter wave plate. Because the transferred polarization is theoretically given by Eq.(13) ($\phi$=π/2), it is possible to compare with the measured results.

Figure 9 shows the measured elements of the Jones vector of the light being measured. The circles and triangles represent the measured points, while the soid lines represent the theoretical curves given by Eq. (13). Figure 9(a) shows the amplitudes of $a_x$ and $a_y$. The measured values agree reasonably well with the theoretical ones. Figure 9(b), on the other hand, shows the phase difference $\alpha$. The measured$\alpha$ is slightly greater than the theoretical value for almost all values of $\theta$. Small discrepancy between measured and theoretical phase difference $\alpha$ is thought to be due to wavelength chirping of the measured light as will be discussed insection 8.4.

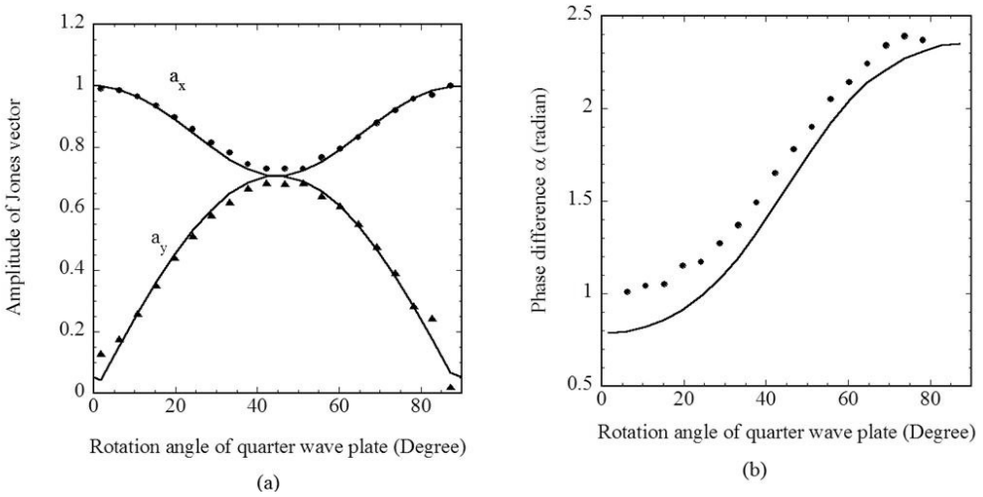


**Figure 9.** Jones vector elements of light being measured with stationary polarization. (a) Amplitudes of the components in the *x*- and *y*-directions. (b) Phase difference between*x*- and *y*-directions. Circles and triangles are measured values. Solid lines are the theoretical values.

The light to be measured is circularly polarized ($a_x = a_y = 1/\sqrt{2}$, $\delta = \pi/2$) at $\theta = \pi/4$, whereas, the lightis linearly polarized along the *x*-axis (i.e., $a_x = 1.0$and, $a_y = 0.0$)at $\theta$= 0 and π/2.

### 8.3. Measurement of time-dependent polarization

The instantaneous polarization when the two light pulses overlap was measured for the cross-TPA. It is thus possible to measure the time-dependent polarization without using high-speed electronics using this method. An optical pulse compressed to 0.9 ps was used for the local oscillation $\hat{\boldsymbol{e}}$ in this measurement. The time resolution is equal to the width of this pulse. The timing of the short reference pulse was scanned over the signal light pulse to trace the variation of the polarization $\hat{\boldsymbol{p}}$of the signal light pulse.

The polarization of the light being measured was varied with time using a polarization-maintaining fiber. The output of the gain-switched LD was made linearly polarized and its

polarization direction was tilted at an angle of 45° relative to the fast and slow axes of the fiber. The propagating optical pulse was separated by the birefringence of the polarization-maintaining fiber since components polarized along the two axes have different the propagation velocities. Consequently, the polarization of the output optical pulse was made time-dependent. A 20-m-long polarization-maintaining fiber imparted a propagation time difference of about 30 ps between the two components.

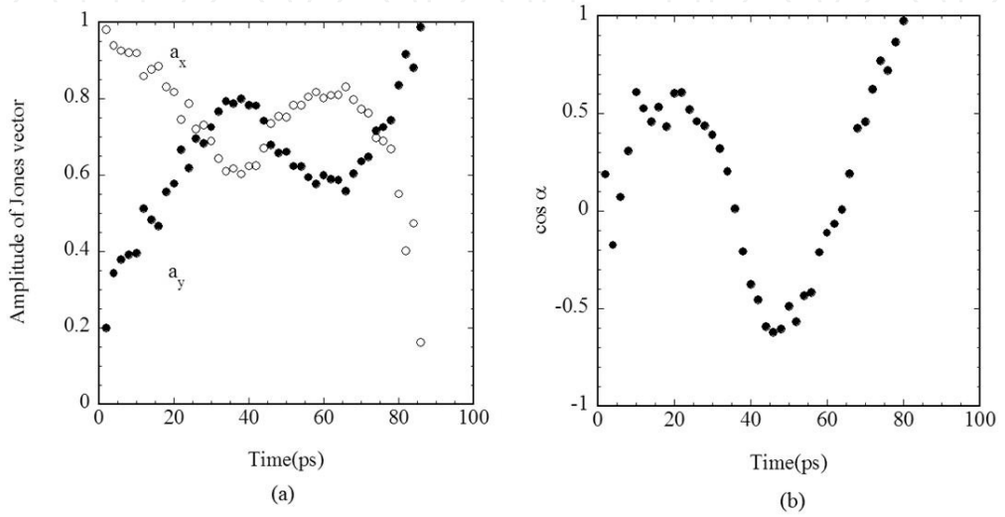


**Figure 10.** Jones vector of the output pulse from a polarization maintaining fiber. (a) amplitude along the x- and y-axes. (b) phase difference.

Figure 10 shows the Jones vector of the output pulse of a polarization maintaining fiber. The x- and y-axes are parallel to the fastand slow axes, respectively. Figure 10(a) shows the measured amplitudes $a_x$ and $a_y$.They vary due to the different group velocities of the polarized light along two axes. The head and tail of output pulse are polarized along the fast and slow axes, respectively. Figure 10(b) shows the measured phase difference $\alpha$. It is determined by the difference in the optical lengths for polarizations along the two axes. It varies with time due wavelength chirping and nonlinear phase shift in the fiber.

### 8.4. Measurement of wavelength chirping

The measured phase difference $\alpha$ between the optical field oscillations along the x- and y-axes is affected by the wavelength chirping. This effect is exploited to measure the wavelength chirping. We consider the case when the linearly polarized signal light is injected to a wave plate whose principal axes are tilted relative the polarization directionof the incident light. The transit times through the wave plate differ by $\Delta T$ for components along the two major axes of the wave plate. For, a $7\lambda/4$ wave plate

$$\Delta T = \pm \frac{7}{4\nu} \tag{38}$$

where $\nu$ is the optical frequency. The linearly polarized light is converted circularly polarized light because the phase shift between polarizations along the two principal axes is$7\pi/2$ which is equivalent to$-\pi/2$.

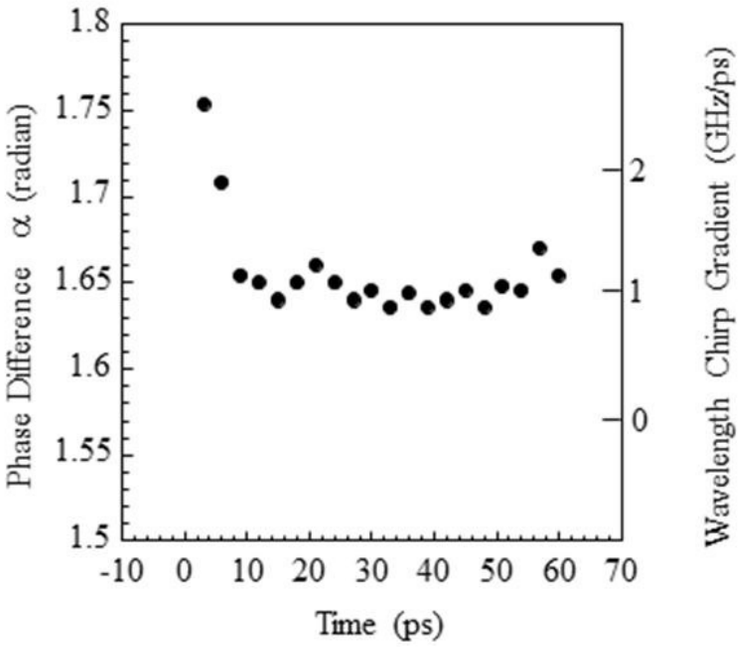


**Figure 11.** Measurement of wavelength chirping of optical pulse from a gain switched LD. The left vertical axis is the phase difference between polarization components along the two principal axes of the wave plate. The right vertical axis is the estimated wavelength chirping gradient.

As the optical frequency is shifted by the wavelength chirping during the time period of $\Delta T$, the optical frequencies of components polarized along the two principal axes after the pulse passes through the wave plate differ by

$$\Delta\nu = \frac{d\nu}{dt}\Delta T \tag{39}$$

where$d\nu/dt$ is the wavelength chirping gradient. The output pulse propagates in free space for a length of $L$ reaching the PD. During the propagation time, polarization components along the two principal axis of the wave plate have different oscillation frequencies. Thus, the optical phase difference $\alpha$ between the two polarization components accumulates during the time period $L/c$, where $c$ is the speed of light. The phase difference at the position of PD is

$$\alpha = -\frac{\pi}{2} \pm 2\pi\Delta\nu\frac{L}{c} \tag{40}$$

The light is, therefore, converted into elliptically polarized light.

Because $\alpha$ can be measured from the TPA of the Si-APD, the wavelength chirping gradient $dv/dt$ can be determined. A $7\lambda/4$ wave plate was used instead of a conventional $\lambda/4$ wave plate to make the phase shift sufficiently large to detect.

Figure 11 shows the measured wavelength chirping of an optical pulse from a gain-switched LD. The linearly polarization is tilted at 45° relative to the principal axis of the $7\lambda/4$ wave plate. The optical pulse passes through the wave plate and propagates in 40-cm of free space.

The chirping gradient $|dv/dt|$ is shown by the left vertical axis in Fig. 11. The measured value is consistent with the wavelength broadening observed by an optical spectrum analyzer. The chirping gradient is large at the head of pulse due to the asymmetry pulse shape.

### 8.5. Measurement of dynamic birefringence of a semiconductor optical amplifier

Semiconductor optical amplifiers (SOAs) generally exhibit birefringence due to the real and/or imaginary parts of the optical gain having different values for transverse electric (TE) and the transverse magnetic (TM) polarizations. The real and imaginary parts of the SOA gain are nonlinear for intense propagating light and induce dynamic birefringence [15,16]. Intense optical pulse affects the polarization of the pulse itself. Consequently, polarization of the output pulse from a SOA varies with time.

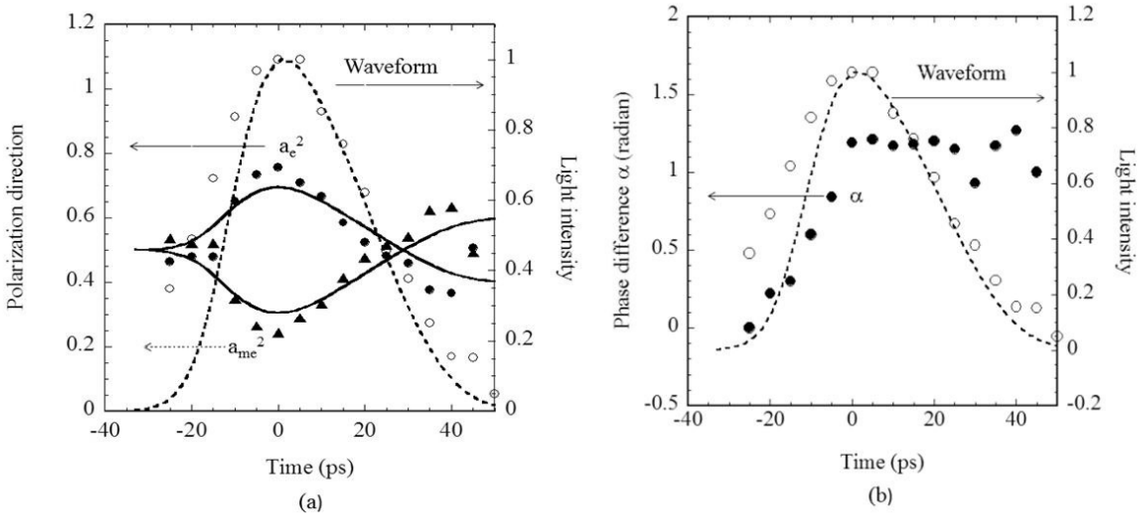


**Figure 12.** Polarization of output pulse from an SOA when the polarization of the input pulse is tilted by 45 ° degree against the x- and y-axes. The waveform of the output pulse is also shown. (a) The closed circles and triangles show the measured polarization directions. The open circles show the measured output waveform. (b) The closed circles show the measured absolute value of phase difference.

A linearly polarized signal light was injected into a SOA witha polarization direction tilted at 45 ° against TE and TM modes. Time dependent Jones vector components of the output pulse from the SOA are measured by the cross-TPA with a reference light pulse with a pulse width of 0.9 ps. The results are shown in Figs. 12(a) and (b). The closed circles and triangles

in Fig. 12(a) show the measured amplitudes $a_e^2$ and $a_m^2$, respectively. $a_e$ and $a_m$are the amplitudes of the Jones vectors for TE and TM polarization. The open circles and dashed line show the measured output pulse shape. The polarization at the head of the pulse is almost the same as that of the injected light pulse. However, the carrier density modulation in the SOA rotates the polarization because the gains for the polarizations of the TE and TM modes have different carrier density dependences. Figure 12(b) shows the measured phase difference $\alpha$. The phase difference varies dynamically due to self-phase modulation in the SOA as a result of the carrier density modulation and spectrum hole burning.

## 9. Conclusions

Photocurrents generated by TPA in PDs were studied. The ratios of nonlinear susceptibility tensor elements were deduced from the polarization dependence of self-TPA for Si- and GaAs-PDs. The photocurrent was isotropic for linear polarization in the Si-PD. On the other hand, TPA is anisotropic and the photocurrent depends on the linear polarization direction in GaAs-PD. The photocurrents for elliptically and circularly polarized light can also be analyzed by the imaginary parts of the nonlinear susceptibility.

The polarization dependence of cross-TPA was measured for a Si-APD. Three types of cross-TPA that are linear-linear, linear-elliptic, and circular-elliptic polarizations were studied. The measured results agree with theoretical values calculated by using parameters obtained from the polarization dependence of self-TPA. These results demonstrate that both self- and cross-TPA can be well described by analysis based on the nonlinear susceptibility tensor.

Cross-TPA was applied to polarization measurements. The Jones vector elements of anarbitrarily polarized signal light can be determined from the four photocurrents generated by cross-TPA between the signal light and the linearly polarized reference light. The time resolution is limited only by the pulse width of the reference light pulse. This measurement method can thus be used to detect rapid polarization variation. It was demonstrated that the polarization of a light pulse from a polarization-maintaining optical fiber and a SOA can be measured by this method.

## Author details

Toshiaki Kagawa*

Address all correspondence to: kagawa@elec.shonan-it.ac.jp

Shonan Institute of Technology, Japan

## References

[1] Kikuchi, K. (1998). Highly sensitive interferometricautocorrelator using Si avalanche photodiode as two-photon absorber. *Electron. Lett.*, 34(1), 123-125.

[2] Wielandy, S., Fishteyn, M., Her, T., Kudelko, D., & Zhang, C. (2002). Real-time measurement of accumulated dispersion for automatic dispersion compensation. *Electron. Lett.*, 38(20), 1198-1199.

[3] Inui, T., Mori, K., Ohara, T., Tanaka, H., Komukai, T., & Morioka, T. (2004). 160 Gbit/s adaptive dispersion equaliser using asynchronous chirp monitor with balanced dispersion configuration. *Electron Lett.*, 40(4), 256-257.

[4] Salem, R., Tudury, G. E., Horton, T. U., Carter, G. M., & Murphy, T. E. (2005). Polarization Insensitive Optical Clock Recovery at 80 Gb/s Using a Silicon Photodiode. IEEE Photon. *Technol. Lett.*, 17(9), 1968-1970.

[5] Butcher, P. N., & Cotter, D. (1990). The Elements of Nonlinear Optics. , Cambridge Studies in Modern Optics: Cambridge University Press.

[6] Boyd, R. W. (2003). *Nonlinear Optics:*, Academic Press.

[7] Dvorak, M. D., Schroeder, W. A., Andersen, D. R., Amirl, A. L., & Wherett, B. S. (1994). Measurement of the Anisotropy of Two-Photon Absorption Coefficients in Zincblende Semiconductors. *IEEE J. Quantum Electron.*, 30(2), 256-268.

[8] Kagawa, T. (2011). Polarization Dependence of Two-Photon Absorption in Si and GaAs Photodiodes at a Wavelength of 1.55 μm. *Jpn. J. Appl. Phys.*, 50, 122203.

[9] Hutchings, D. C., & Wherett, B. S. (1994). Theory of anisotropy of two-photon absorption in zinc-blende semiconductors. *Phys. Rev. B*, 49(4), 2418-2426.

[10] Murayama, M., & Nakayama, T. (1995). Ab initio calculation of two-photon absorption spectra in semiconductors. *Phys. Rev.B*, 52(7), 4986-4995.

[11] Yu, P. T., & Cardona, M. (2005). Fundamentals of Semiconductors, 3 rd ed.:Springer.

[12] Cardona, M., & Pollak, F. H. (1966). Energy-Band Structure of Germanium and Silicon: The kp Method. *Phys. Rev.*, 142(2), 530-543.

[13] Kagawa, T., & Ooami, S. (2007). Polarization dependence of two-photon absorption in Si avalanche photodiode. *Jpn. J. Appl. Phys.*, 46(2), 664-668.

[14] Kagawa, T. (2008). Measurement of Constant and Time-Dependent Polarizations Using Two-Photon Absorption of Si Avalanche Photodiode. *Jpn. J. Appl. Phys.*, 47(3), 1628-1631.

[15] Dorren, H. J. S., Lenstra, D., Liu, T., Hill, T., & Khoe, G. D. (2003). Nonlienar Polarization Rotation in Semiconductor Optical Amplifiers: Theory and Application to All-Optical Flip-Flop Memories. *IEEE J. Quantum Electron.*, 30(1), 141-148.

[16] Takahashi, Y., Neogi, A., & Kawaguchi, H. (1998). Polarization-Dependent Nonlinear Gain in Semiconductor Lasers. *IEEE J. Quantum Electron.*, 34(9), 1660-1672.



IntechOpen